

# Interconversion between Rare-Earth Metal(III) Chromates(V) and Low-Crystalline Phases by Reduction with Methanol and Oxidation in Air

Yoshitaka Aoki,\* Hiroki Habazaki, and Hidetaka Konno

Division of Materials Science and Engineering, Graduate School of Engineering,  
Hokkaido University, Sapporo, 060-8628 Japan

Received October 9, 2002. Revised Manuscript Received February 6, 2003

Rare-earth metal(III) chromates(V),  $\text{LaCrO}_4$ ,  $\text{NdCrO}_4$ , and  $\text{Y}_{0.9}\text{CrO}_{3.85}$ , were found to show reversible structural changes by reduction with methanol and oxidation in air. This anomalous behavior was investigated by X-ray diffraction, X-ray photoelectron spectroscopy, Fourier transform infrared, in situ Raman spectroscopy, and other methods. After less than 30 min of reduction at 543 K, zircon-type  $\text{NdCrO}_4$  in the bulk scale changed to the low-crystalline II-KDP-type phase, which has the same arrangement of metal atoms as zircon. The reduced phase was quickly reverted to the zircon-type phase by air oxidation at 543 K for a few minutes.  $\text{NdCrO}_4$  was reduced by hydrogen from methanol by forming hydrogen bonds between  $\text{CrO}_4$  units, which caused the oxygen displacement and the formation of pseudo-octahedral  $\text{CrO}_{6-m}(\text{OH})_m$  units, leading to the distorted II-KDP-type structure. Defect zircon-type  $\text{Y}_{0.9}\text{CrO}_{3.85}$  changed more quickly to the low-crystalline II-KDP-type phase than  $\text{NdCrO}_4$ , and the structure was not completely restored by the oxidation at 543 K for 1 h, because of the formation of small amounts of  $\text{YCrO}_3$  and  $\text{Cr}_2\text{O}_3$ . Monazite-type  $\text{LaCrO}_4$  changed to an amorphous phase with the formation of the Schottky defects of oxide ions because of the structural differences between the monazite-type and II-KDP-type phases and was restored by air oxidation at 723 K.

## Introduction

Chromate(V) has attracted interest because of its roles in Cr-induced calcinogenesis<sup>1–4</sup> and oxidation of organic substrates by Cr(VI).<sup>5–7</sup> For example, the  $\text{Cr}^{\text{VO}_4^{3-}}$  species formed by the reduction of  $\text{Cr}^{\text{VI}}\text{O}_4^{2-}$  species directly oxidize ribose and are involved in DNA lesions,<sup>1,2,4</sup> and Cr(V) catalyzes the epoxidation of various olefins.<sup>5,6</sup> In addition, it is also known that the  $\text{CrO}_4^{3-}$  species are formed on various chromia catalysts through catalytic processes.<sup>8,9</sup> One of the reasons for the reactivities of chromate(V) is the high redox potential of Cr(III)/Cr(V), which is estimated to be 1.32 V vs SHE in acidic media.<sup>10</sup> The reactivity of chromate(V) compounds, such as  $\text{Li}_3\text{CrO}_4$  and  $\text{K}_3\text{CrO}_8$ , however, has not

been reported because these compounds are not stable in the ambient atmosphere as a result of the electronic configuration of Cr(V) ions,  $d^1$ . Exceptionally, rare-earth metal(III) chromates(V),  $\text{RECrO}_4$  [RE: rare-earth metal(III)], are stable at elevated temperatures in air.<sup>11–14</sup> There are a number of reports on the structure and magnetic properties due to the two magnetic ions, Cr(V) and RE(III), in  $\text{RECrO}_4$ ,<sup>15–21</sup> but reactivities, such as the catalytic and redox activities, have not been investigated. Therefore, it would be of value to investigate the properties of  $\text{RECrO}_4$  in catalytic oxidation of organic compounds.

It has been reported<sup>11,12,16–22</sup> that  $\text{LaCrO}_4$  has a monazite-type structure (monoclinic,  $P2_1/n$ ) and  $\text{RECrO}_4$  compounds of RE = Nd–Lu and Y have zircon-type structure (tetragonal,  $I4_1/amd$ ). Recently, we have synthesized these compounds a phase by pyrolysis

\* To whom correspondence should be addressed. Present address: Topochemical Design Laboratory, Frontier Research System, Institute of Physics and Chemistry, RIKEN, 2-1 Hirosawa, Wako, Saitama, 351-0198 Japan. Tel: +81-48-462-1111 ext. 6315. Fax: +81-48-467-9599. E-mail: yaoki@postman.riken.go.jp.

(1) Bose, R. N.; Fonkeng, S.; Moggaddas, S.; Stroup, D. *Nucleic Acids Res.* **1998**, *26*, 1588.  
(2) Ferrell, R.; Judd, R.; Lay, P.; Dixon, N.; Baker, R.; Bonin, A. *Chem. Res. Toxicol.* **1988**, *1*, 101.  
(3) Brauer, S. I.; Wetterhahn, K. *J. Am. Chem. Soc.* **1991**, *113*, 3001.  
(4) Codd, R.; Lay, P. A. *J. Am. Chem. Soc.* **1999**, *121*, 7864.  
(5) Samsel, E. G.; Srinivasan, K.; Kochi, J. K. *J. Am. Chem. Soc.* **1985**, *107*, 7606.  
(6) Siddall, T. L.; Miyaura, N.; Kochi, J. K. *J. Chem. Soc., Chem. Commun.* **1983**, 1185.  
(7) Gould, E. *Acc. Chem. Res.* **1986**, *19*, 66.  
(8) Weckhuysen, B. M.; Wachs, I. E.; Schoonheydt, R. A. *Chem. Rev.* **1996**, *96*, 3327.  
(9) Cordischi, D.; Campa, M. C.; Indovian, V.; Occhiazzi, M. *J. Chem. Soc., Faraday Trans.* **1994**, *90*, 207.  
(10) Ghosh, M. C.; Gould, E. S. *J. Am. Chem. Soc.* **1993**, *115*, 3167.

(11) Schwarz, H. Z. *Anorg. Allg. Chem.* **1963**, *322*, 1.  
(12) Schwarz, H. Z. *Anorg. Allg. Chem.* **1963**, *323*, 275.  
(13) Doile, W. P.; Pryde, I. J. *J. Inorg. Nucl. Chem.* **1976**, *38*, 733.  
(14) Furusaki, A.; Konno, H.; Furuichi, R. *Nippon Kagaku Kaishi* **1992**, 612.  
(15) Walter, H.; Kahle, G.; Mulder, K.; Schopper, C.; Schwarz, H. *Int. J. Magn.* **1973**, *5*, 129.  
(16) Buisson, G.; Tcheou, F.; Sayetat, F.; Scheuermann, K. *Solid State Commun.* **1976**, *18*, 871.  
(17) Steiner, M.; Dachs, H.; Ott, H. *Solid State Commun.* **1979**, *29*, 231.  
(18) Jiménez, E.; Isasi, J.; Sáez-Puche, R. *J. Alloys Compd.* **2000**, *312*, 53.  
(19) Jiménez, E.; Isasi, J.; Sáez-Puche, R. *J. Alloys Compd.* **2001**, *323–324*, 115.  
(20) Tezuka, K.; Hinatsu, Y. *J. Solid State Chem.* **2001**, *160*, 362.  
(21) Tezuka, K.; Doi, Y.; Hinatsu, Y. *J. Mater. Chem.* **2002**, *12*, 1189.  
(22) Manca, S. G.; Baran, E. J. *J. Phys. Chem. Solid* **1981**, *42*, 923.

of the precursors prepared from mixed solutions of Cr(VI) and RE(III) and refined the crystal structure by Rietveld analysis.<sup>23–27</sup> For the compounds of RE(III) ions smaller than the Gd(III) ion, these compounds can be obtained as a single phase only when  $0.85 < \text{RE(III)}/\text{Cr(V)} < 0.95$  and the composition is  $\text{RE}_{0.9}\text{CrO}_{3.85}$  or very close to this.<sup>22</sup> They are defect zircon-type with both RE(III) and oxygen defects and different from the structures reported so far.

In a series of experiments, we have attempted to effect catalytic oxidation of *n*-butane and various alcohols at 543 K using a polycrystalline powder of  $\text{NdCrO}_4$ . In these experiments, it was observed that the zircon-type structure of this oxide broke down and Cr(V) was reduced to Cr(III) by organic compounds (confirmed by X-ray diffraction (XRD), X-ray photoelectron spectroscopy (XPS), and Raman spectroscopy) but that a short period of oxidation in air restored the structure including Cr(V). These reversible reactions are unexpected because the stable Cr(III) states generated by the reduction of the Cr(V) compound easily returned to the unstable Cr(V) state and because quick recrystallization occurred in a bulk scale under mild oxidation conditions. The present work investigated the redox reactions and structure changes of  $\text{LaCrO}_4$  (monazite-type),  $\text{NdCrO}_4$  (zircon-type), and  $\text{Y}_{0.9}\text{CrO}_{3.85}$  (defect zircon-type) by methanol vapor and air by XRD, XPS, Fourier transform infrared (FT-IR) spectroscopy, chemical analysis, thermal gravimetry (TG), superconducting quantum interference device (SQUID), and in situ Raman spectroscopy.

## Experimental Section

Single-phase rare-earth metal(III) chromates(V) were synthesized by pyrolysis of the precursor at 873 K for 1 h in air for  $\text{LaCrO}_4$ , at 853 K for 3 h in  $\text{O}_2$  for  $\text{NdCrO}_4$ , and at 843 K for 10 d in  $\text{O}_2$  for  $\text{Y}_{0.9}\text{CrO}_{3.85}$ . The precursors were prepared from the stoichiometric solutions of  $\text{RE}(\text{CH}_3\text{COO})_3 \cdot n\text{H}_2\text{O}$  (RE = La, Nd, or Y) and  $\text{CrO}_3$ , with metal concentrations being determined by chelatometry and redox titration.<sup>14,23,24</sup> The methods of synthesis and the detailed structure of polycrystalline samples are described elsewhere.<sup>14,23,24</sup> The composition and purity of the samples were determined by titration, XPS, XRD, and others.<sup>14,23–25</sup> The titration procedure was the same as that in ref 14. The specific surface area of the sample powder was measured by nitrogen adsorption (Brunauer–Emmett–Teller method) at 77 K.

The reaction of the three compounds with methanol was carried out in a continuous-flow tubular fixed-bed reactor of a quartz tube (7.0 mm in diameter) connected to a gas chromatograph (GC) system; 50 mg of a sample powder was used as a reactant. Before the reaction, the sample temperature was raised at  $10 \text{ K min}^{-1}$  to 543 K and maintained at 543 K for 1 h in an Ar (99.99% pure) flow of  $100 \text{ cm}^3 \text{ min}^{-1}$ . Then, the experiment was started by flowing 10 vol % methanol/Ar gas through the sample at  $100 \text{ cm}^3 \text{ min}^{-1}$ . The methanol gas was generated by bubbling Ar in methanol and diluted to 10 vol % with pure Ar. At the end of the reaction, reactant gas was replaced by Ar gas, and the sample was cooled at  $50 \text{ K min}^{-1}$  to room temperature in an Ar atmosphere. The sample was

kept in the reactor until the temperature was reached below 373 K. After the reaction with methanol, the samples were oxidized by dry air in the same reactor. In other experiments, a 1 h reduction by methanol and oxidation by air were carried out consecutively at 543 K by changing the flow of 10 vol % methanol/Ar to dry air at  $100 \text{ cm}^3 \text{ min}^{-1}$ . At the end of the oxidation, the sample was immediately taken out of the reactor and kept in a desiccator.

The reaction with other alcohols, such as ethanol, cyclohexanol, and butanol, and *n*-butane was also carried out likewise. The compounds were reacted at 543 K for 3 h in the  $\text{N}_2$  gas saturated with the alcohol or in the 10 vol % *n*-butane/ $\text{N}_2$  gas. In other experiments, the 3-h-reacted samples were heated at 543 K for 1 h in air. The zircon-type  $\text{NdVO}_4$  (Nakarai Kagaku, Japan) and  $\text{CaCr}^{\text{VI}}\text{O}_4$  (Kanto Kagaku, Japan) were also reacted with methanol by flowing methanol-saturated  $\text{N}_2$  gas at 623 K for 24 h.

The XRD patterns were measured by a Rigaku Geigerflex diffractometer with a monochromator under the conditions  $\text{Cu K}\alpha$ , 40 kV, 25 mA, and scanning step  $0.02^\circ$  ( $2\theta$ ). The XPS measurements were carried out by a VG ESCALAB MkII. The temperature dependence of the magnetic susceptibility was measured at 1000 G by a Quantum Design SQUID magnetometer under zero-field-cooled conditions in the temperature range 20–300 K. Details of these measurements are described elsewhere.<sup>23,24,28</sup> The FT-IR spectra were recorded for pellet samples pressed with KBr by a Jasco FT/IR203 spectrometer at room temperature.

The valence of chromium in the samples reacted with methanol for 1 h was determined by chemical analysis. TG analysis of the sample reacted with methanol for 1 h was carried out in a Seiko Instruments TG/DTA32 in flowing air at  $10 \text{ K min}^{-1}$ .

During the reaction with methanol and oxidation by air, in situ Raman spectroscopic measurements were carried out by a Jasco TRS-401 with a triple-type monochromator under the irradiation of an Ar laser (514.5 nm line). The laser power was adjusted to 2 mW at the probe to prevent overheating of the sample. The laser beam was irradiated on the sample by the incident angle of  $55^\circ$ , and the backscattered light was detected by a Princeton LN/CCD detector. A specially designed optical cell was employed for the in situ experiments. The cell was smaller than  $40 \text{ cm}^3$  and equipped with an electronic furnace and a line of cooling water to acquire the spectra under the controlled atmosphere and temperature. The 50 mg sample powder was put in a quartz cup and set in the electronic furnace. The sample temperature was measured by a Pt/Rh thermocouple attached to the quartz cup.

## Results and Discussion

**Reversible Structure Changes of Rare-Earth Metal(III) Chromates(V).** The synthesized samples were confirmed to be single phase by XRD. The compositions by titration were  $\text{Nd}_{0.994}\text{Cr}_{1.00}\text{O}_{3.99}$ ,  $\text{Y}_{0.897}\text{Cr}_{1.00}\text{O}_{3.86}$ , and  $\text{La}_{0.997}\text{Cr}_{1.00}\text{O}_{3.99}$ , indicating that a nominal valence number of the Cr atom in these compounds was five. Hereafter, these compounds are referred to as  $\text{NdCrO}_4$ ,  $\text{Y}_{0.9}\text{CrO}_{3.85}$ , and  $\text{LaCrO}_4$ . The electron spin resonance spectra of  $\text{LaCrO}_4$ <sup>14</sup> and  $\text{Y}_{0.9}\text{CrO}_{3.85}$ <sup>24</sup> showed only the typical bands of  $\text{Cr}^{\text{V}} \text{d}^1$  compounds and did not show those assigned to Cr(II) or Cr(III) species. The Cr 2p XPS spectra of  $\text{LaCrO}_4$  and  $\text{NdCrO}_4$  were also typical for Cr(V) compounds (the spectrum cited from ref 23 is shown in Figure 4).<sup>23,28</sup> Further, as will be mentioned below, the strong  $\nu_1$  (symmetric-stretching) mode of  $\text{Cr}^{\text{VI}}\text{O}_4^{2-}$ <sup>25</sup> was not observed in the Raman spectra of any compounds. From these results, it is evident that

(23) Aoki, Y.; Konno, H.; Tachikawa, H.; Inagaki, M. *Bull. Chem. Soc. Jpn.* **2000**, *73*, 1197.

(24) Aoki, Y.; Konno, H. *J. Mater. Chem.* **2001**, *11*, 1458.

(25) Aoki, Y.; Konno, H. *J. Solid State Chem.* **2001**, *156*, 370.

(26) Aoki, Y.; Konno, H.; Tachikawa, H. *J. Mater. Chem.* **2001**, *11*, 1214.

(27) Konno, H.; Aoki, Y.; Klenscár, Z.; Vértés, A.; Wakeshima, M.; Tezuka, K.; Hinatsu, Y. *Bull. Chem. Soc. Jpn.* **2001**, *74*, 2335.

(28) Konno, H.; Tachikawa, H.; Furusaki, A.; Furuichi, R. *Anal. Sci.* **1992**, *8*, 641.

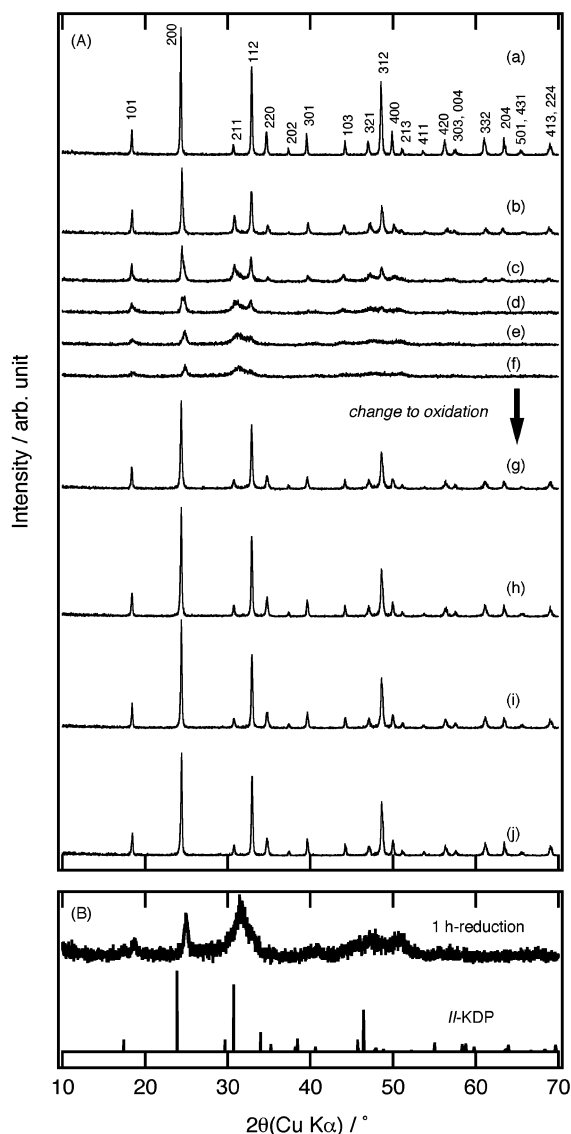


**Figure 1.** (A) XRD patterns of  $\text{NdCrO}_4$  reduced with methanol at 543 K for (a) 0 min (as-prepared), (b) 5 min, (c) 10 min, (d) 20 min, (e) 30 min, and (f) 1 h and then oxidized at 543 K for (g) 3 min, (h) 5 min, (i) 10 min, and (j) 1 h in air. (B) XRD pattern of  $\text{NdCrO}_4$  reacted with methanol at 543 K for 1 h and the calculated pattern of II-KDP.

the as-prepared samples were single-phase rare-earth metal(III) chromates(V). The specific surface areas of polycrystalline  $\text{NdCrO}_4$ ,  $\text{Y}_{0.9}\text{CrO}_{3.85}$ , and  $\text{LaCrO}_4$  were 4.0, 3.5, and 4.1  $\text{m}^2 \text{g}^{-1}$ , respectively. All of the compounds are monooxochromate salts; the  $\text{Cr}^{\text{V}}\text{O}_4^{3-}$  tetrahedra have  $C_1$  symmetry with four different Cr–O bond lengths in  $\text{LaCrO}_4$  and  $D_{2d}$  symmetry with four equivalent Cr–O bonds in  $\text{NdCrO}_4$ , as reported previously.<sup>23</sup> The defect zircon-type  $\text{Y}_{0.9}\text{CrO}_{3.85}$  has a structure similar to that of  $\text{NdCrO}_4$  but contains  $\text{CrO}_3^-$  with a dangling bond created by O deficits, forming  $\text{Cr}_2\text{O}_7^{4-}$  dimers by sharing an oxygen atom with the adjacent  $\text{CrO}_4$  tetrahedra.<sup>24</sup>

The XRD pattern of as-prepared  $\text{NdCrO}_4$  is shown in part a of Figure 1A, and all peaks were indexed to the zircon-type. Parts b–f of Figure 1A show that by the reaction with methanol at 543 K in an Ar atmosphere the peak broadens and there is a decrease in intensity with increasing reaction time; after 20 min most of the

strong peaks disappeared, indicating a degradation of the zircon-type structure. These changes were less pronounced after 30 min and the diffraction pattern could not be identified, indicating that the zircon-type  $\text{NdCrO}_4$  transformed to low-crystalline, new phases by the reaction with methanol for 30 min. The color of the  $\text{NdCrO}_4$  powder changed from dark green to grayish green after 1 h. The specific surface area of  $\text{NdCrO}_4$  did not change after 1 h of reaction, so these changes in XRD patterns were not caused by pulverization or disintegration. As shown in parts g–j of Figure 1A, however, the degraded structure of  $\text{NdCrO}_4$  (part f of Figure 1A) was restored by oxidation at 543 K in air. The restoration of the structure took place very quickly; samples oxidized for 3 min exhibited sharp peaks of a zircon-type phase, and oxidation for more than 10 min completely restored the original  $\text{NdCrO}_4$  structure. This suggests that the rearrangement of metal atoms during the reduction took place in a very short range. Figure 1B will be discussed later.

As mentioned before, the XPS spectrum of Cr 2p for as-prepared  $\text{NdCrO}_4$  was typical for Cr(V) compounds, having sharp peaks of  $2p_{3/2}$  at 579 eV and  $2p_{1/2}$  at 588 eV,<sup>28</sup> while the spectrum of the reacted sample f in Figure 1A was that assigned to the Cr(III) compound,  $2p_{3/2}$  at 576 eV and  $2p_{1/2}$  at 586 eV.<sup>29</sup> Thus, the structural degradation is accompanied by a reduction of Cr(V) to Cr(III). The results by XPS are confined to the surface, but as described in the next section, Cr(V) ions in the bulk were also reduced by the reaction with methanol.

The XRD patterns of defect zircon-type  $\text{Y}_{0.9}\text{CrO}_{3.85}$  reacted with methanol are shown in parts a–e of Figure 2A. It is clear that  $\text{Y}_{0.9}\text{CrO}_{3.85}$  also degrades by reduction with methanol. Similar to  $\text{NdCrO}_4$ , most of the diffraction peaks of  $\text{Y}_{0.9}\text{CrO}_{3.85}$  disappeared and an alternative pattern was obtained. In this case, the compound changed to low-crystalline phases by 5 min of reaction, and after that the XRD pattern did not change markedly up to 1 h, showing that the change in  $\text{Y}_{0.9}\text{CrO}_{3.85}$  is faster than that in  $\text{NdCrO}_4$ . The specific surface area of  $\text{Y}_{0.9}\text{CrO}_{3.85}$  also did not change. The XRD patterns of the sample reacted with methanol for 1 h and then oxidized at 543 K in air are shown in parts f–i of Figure 2A. It is seen that the restoration of the defect zircon-type structure to the original crystalline state was not very rapid. Figure 2B will be discussed later, together with Figure 1B.

The results of similar experiments with monazite-type  $\text{LaCrO}_4$  are shown in Figure 3. The structural changes of  $\text{LaCrO}_4$  were quite different from those of the zircon-type compounds. Peak intensities decreased monotonically, and the XRD pattern became an amorphous type after 2 h of reaction. As shown in Figure 3h, this aperiodic phase was not restored to a crystalline phase by the oxidation at 543 K for 1 h in air, but it was restored to the original structure at 723 K, as shown in part i.

**Phases Formed by the Reduction of  $\text{NdCrO}_4$ ,  $\text{Y}_{0.9}\text{CrO}_{3.85}$ , and  $\text{LaCrO}_4$ .** As shown in Figure 4, the XPS spectra revealed that the surface of the reduced  $\text{NdCrO}_4$  was composed of Cr(III) species. To examine

(29) Gazzoli, D.; Occhiuzzi, M.; Chimino, A.; Minelli, G.; Varigi, M. *Surf. Interface Anal.* **1992**, *18*, 315.



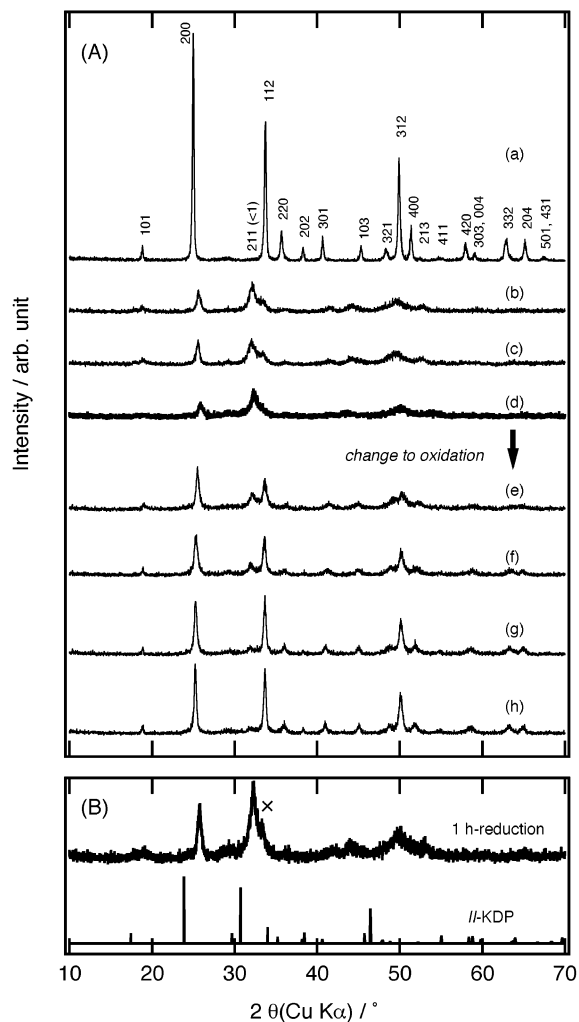
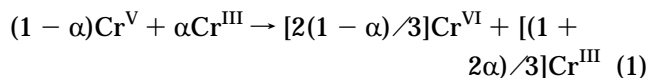


**Figure 2.** (A) XRD patterns of  $Y_{0.9}CrO_{3.85}$  reduced with methanol at 543 K for (a) 0 min (as-prepared), (b) 5 min, (c) 10 min, and (d) 1 h and then oxidized at 543 K for (e) 3 min, (f) 10 min, (g) 30 min, and (h) 1 h in air. (B) XRD pattern of  $Y_{0.9}CrO_{3.85}$  reacted with methanol at 543 K for 1 h and the calculated pattern of II-KDP. The peak shown by  $\times$  is referred to in the text.

the valence state of Cr ions in the reduced phases, redox titration was carried out for the samples reacted with methanol at 543 K for 1 h. About 1 g of the samples was dissolved in 100 cm<sup>3</sup> of a 2 mol dm<sup>-3</sup> H<sub>2</sub>SO<sub>4</sub> solution at 80 °C, and this resulted in the disproportionation of Cr(V) into Cr(III)/Cr(VI) = 1/2, which was confirmed by using as-prepared samples. Assuming that the Cr ions in the samples are only Cr(III) and Cr(V) and that a mole fraction of Cr(III) is  $\alpha$ , the reduced phase dissolves into a sulfuric acid solution as follows:



Because the concentration of Cr(VI) can be determined by the redox titration and the total amount of Cr in the sample is known, the Cr(III)/Cr(V) mole ratio and the average valence of Cr ions in the reduced phases can be calculated. They are shown in Table 1. To confirm the assumption that only Cr(III) and Cr(V) were present, the effective magnetic moments on the Cr ions were

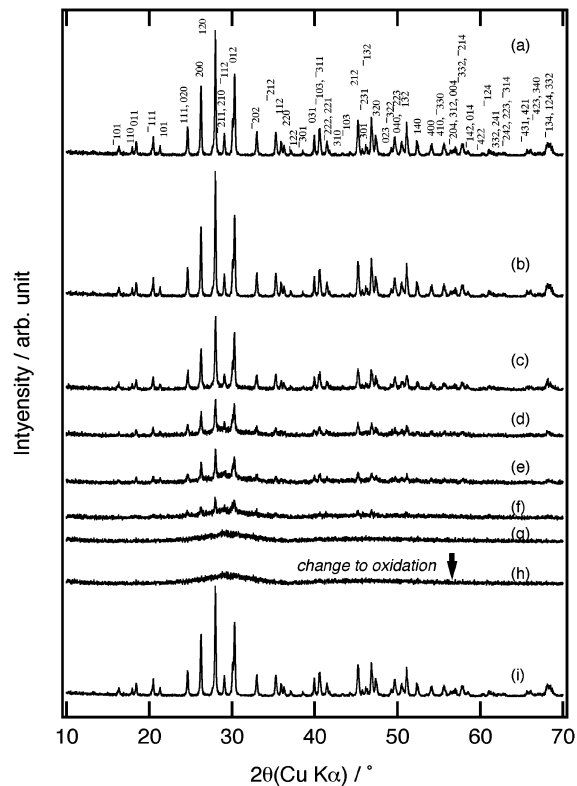


**Figure 3.** XRD patterns of  $LaCrO_4$  reduced with methanol at 543 K for (a) 0 min (as-prepared), (b) 5 min, (c) 10 min, (d) 20 min, (e) 30 min, (f) 1 h and (g) 2 h and then oxidized (h) at 543 K for 1 h in air or (i) at 673 K.

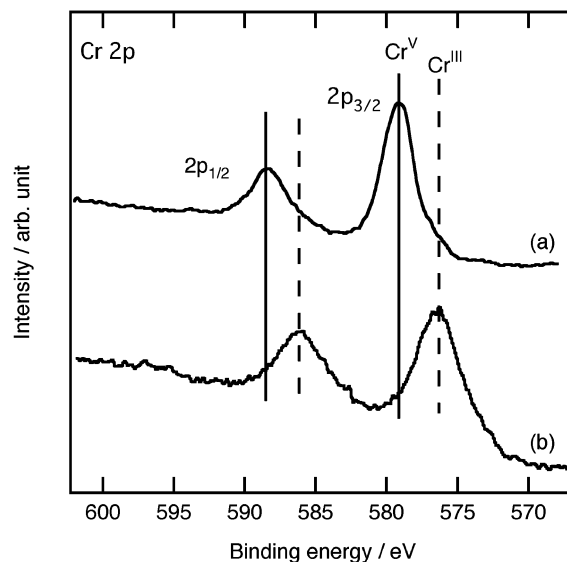


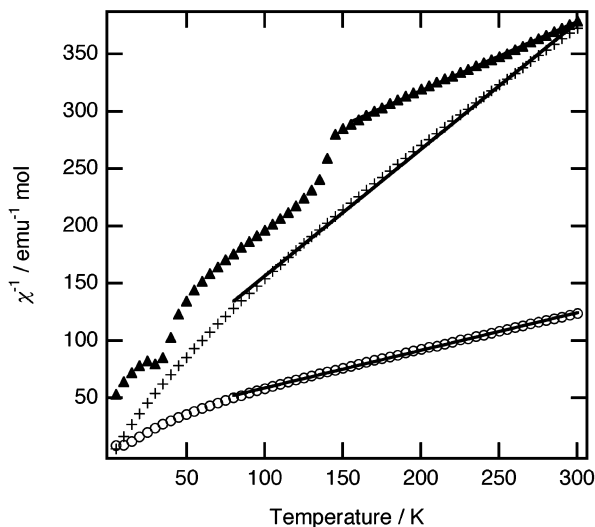
**Figure 4.** Cr 2p XPS spectra of  $NdCrO_4$ : (a) as-prepared and (b) reacted with methanol at 543 K for 1 h in an inert atmosphere.

measured. The reciprocal of the magnetic susceptibility,  $\chi^{-1}$ , of the reduced phases was plotted as a function of temperature in Figure 5. The reduced  $NdCrO_4$  and  $LaCrO_4$  showed the downward deviation of the  $\chi^{-1}-T$  plots below 50 K because of the antiferromagnetic transition of the residual chromate(V) compounds<sup>26</sup> and obeyed the Curie-Weiss law above 80 K. The reduced  $Y_{0.9}CrO_{3.85}$  also obeyed the Curie-Weiss law above 150 K, but two gaps were observed on the curve at around 50 and 140 K. The gap at around 140 K may be due to

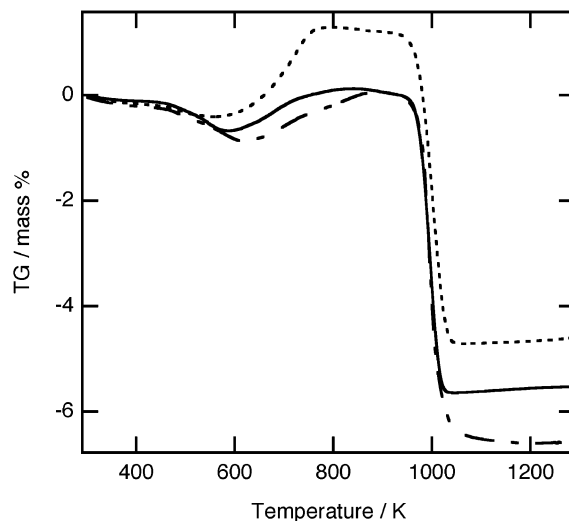
**Table 1. Results of the Redox Titration and Magnetic Measurements for Samples Reacted with Methanol at 543 K for 1 h**

	NdCrO <sub>4</sub>	Y <sub>0.9</sub> CrO <sub>3.85</sub>	LaCrO <sub>4</sub>
As prepared			
average valence of Cr	3.52	3.00	4.28
mole ratio of Cr <sup>III</sup> /Cr <sup>V</sup>	74/26	100/0	36/64
Reduced phase			
observed			
total, $\mu_{\text{tot}}^{\circ}$	4.93	<i>a</i>	<i>a</i>
Cr part, $\mu_{\text{Cr}}^{\circ}$	3.35	3.78	2.67
theoretical			
Cr part, $\mu_{\text{Cr}}^{\text{t}}$	3.44	3.87	2.68

<sup>a</sup>  $\mu_{\text{tot}}^{\circ}$  values of LaCrO<sub>4</sub> and Y<sub>0.9</sub>CrO<sub>3.85</sub> correspond to  $\mu_{\text{Cr}}^{\circ}$  values because La<sup>III</sup> and Y<sup>III</sup> have no spin ( $s = 0$ ) and so have no contribution to the magnetic moment of compounds.

**Figure 5.** Reciprocal of the magnetic susceptibility,  $\chi$ , for the reduced NdCrO<sub>4</sub> (○), Y<sub>0.9</sub>CrO<sub>3.85</sub> (▲), and LaCrO<sub>4</sub> (+) as a function of temperature.

the antiferromagnetic transition of YCrO<sub>3</sub>, which is reported to occur at  $T_N = 141$  K.<sup>30</sup> Although the peaks that can be assigned to YCrO<sub>3</sub> were not found in the Raman spectra of the reduced Y<sub>0.9</sub>CrO<sub>3.85</sub>, which are shown in the next section, a weak shoulder peak at around 32°, shown by × in Figure 2B, corresponds to the 121 of perovskite-type YCrO<sub>3</sub>.<sup>31</sup> It is, however, difficult to explain the gap around 50 K at present because Cr(III) and Cr(V) compounds that satisfy this magnetic property are not found. The observed magnetic moments of Cr ions,  $\mu_{\text{Cr}}^{\circ}$ , are listed in Table 1, where the value for the reduced NdCrO<sub>4</sub> was obtained by correcting the total magnetic moment,  $\mu_{\text{tot}}^{\circ}$ , with the contribution from Nd(III),  $\mu_{\text{Nd}}^{\text{t}} = 3.68 \mu_{\text{B}}$ .<sup>32</sup> Theoretical magnetic moment values,  $\mu_{\text{Cr}}^{\text{t}}$ , were calculated by using the theoretical magnetic moments of Cr(III) (3.87  $\mu_{\text{B}}$ ) and Cr(V) (1.73  $\mu_{\text{B}}$ )<sup>32</sup> and the Cr(III)/Cr(V) mole ratio in Table 1. The values of  $\mu_{\text{Cr}}^{\circ}$  are in agreement with  $\mu_{\text{Cr}}^{\text{t}}$ , indicating that the valence state of Cr ions in the reduced phases are only Cr(III) and Cr(V). Accordingly, it is concluded that almost all of the Cr(V) ions in Y<sub>0.9</sub>CrO<sub>3.85</sub> were reduced to the trivalent state, while a part of the Cr(V) ions remained in the reduced NdCrO<sub>4</sub> and

**Figure 6.** Results of TG analysis of the reduced NdCrO<sub>4</sub> (—), Y<sub>0.9</sub>CrO<sub>3.85</sub> (---), and LaCrO<sub>4</sub> (- · -) in air. The reduced phases were prepared by reduction with methanol at 543 K for 1 h.

LaCrO<sub>4</sub>. These results clearly indicate that rare-earth metal(III) chromates(V) are reduced to Cr(III) in the bulk scale by the reaction with methanol at 543 K.

By TG analysis in air, the mass of the reduced phases changed, as shown in Figure 6. For all samples, the products at 800 K were identified by XRD as crystalline rare-earth metal(III) chromates(V), indicating that the amorphous phase of LaCrO<sub>4</sub> can also be restored to the crystalline phase by annealing at elevated temperatures, as mentioned above. The slight mass loss below ca. 470 K in all samples can be attributed to the loss of adsorbed water. The large mass loss from 940 K and the plateaus above 1030 K are due to the formation of perovskite-type chromite(III) compounds by release of oxygen. After liberation of water below 470 K, the reduced LaCrO<sub>4</sub> showed only a small mass loss in a 500–600 K range. The large mass gain above 600 K and the plateau in the 760–940 K range are attributed to the formation of LaCrO<sub>4</sub> by oxidation of Cr(III) to Cr(V). The mass change of the reduced zircon-type compounds was quite different from the reduced LaCrO<sub>4</sub>. The reduced NdCrO<sub>4</sub> showed further mass loss above 470 K; there was a minimum around 600 K, after which the mass increased to nearly the original mass at around 700 K. As the reduced phase has transformed to zircon-type NdCrO<sub>4</sub> at 700 K, this indicates that the net mass of the NdCrO<sub>4</sub> sample does not change very much by reduction with methanol. Accordingly, the reduction of NdCrO<sub>4</sub> with methanol does not form Schottky-type defects in the oxide ions. The mass change of the reduced Y<sub>0.9</sub>CrO<sub>3.85</sub> was similar to that of the reduced NdCrO<sub>4</sub>, but the mass gain was slow and continued to around 880 K. This result is consistent with Figure 2 in that the conversion of the reduced Y<sub>0.9</sub>CrO<sub>3.85</sub> to the original defect zircon-type phase was not accomplished by 1 h of oxidation at 543 K. Elemental analysis by a combustion method indicated that the reduced phases of NdCrO<sub>4</sub>, Y<sub>0.9</sub>CrO<sub>3.85</sub>, and LaCrO<sub>4</sub> contained 0.5, 0.7, and 0.1 mass % of hydrogen, respectively, but no carbon or nitrogen. These results offer the possibility that the reduction of NdCrO<sub>4</sub> and Y<sub>0.9</sub>CrO<sub>3.85</sub> is caused by hydrogen.

(30) Judin, V. M.; Sherman, A. B. *Solid State Commun.* **1966**, *4*, 661.

(31) JCPDS 34-0365.

(32) Yamaguchi, T.; Yanagida, H. *Magnetoceramics*; Gihodo: Tokyo, 1985; pp 24 and 25.

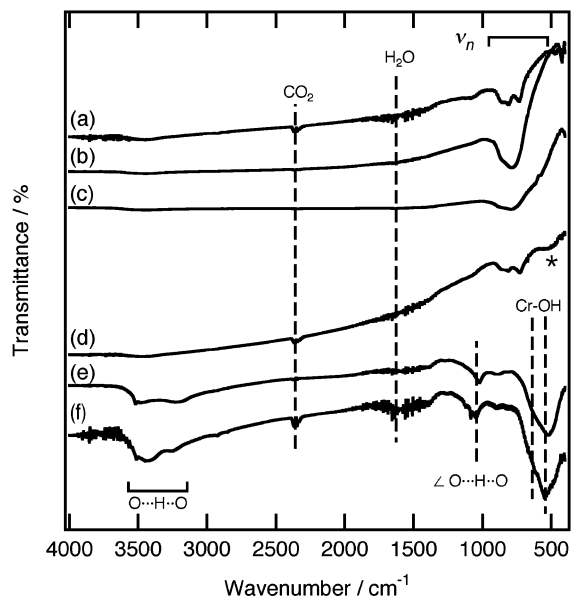


**Figure 7.** FT-IR spectra of as-prepared (a)  $\text{LaCrO}_4$ , (b)  $\text{NdCrO}_4$ , and (c)  $\text{Y}_{0.9}\text{CrO}_{3.85}$  and the reduced phase of (d)  $\text{LaCrO}_4$ , (e)  $\text{NdCrO}_4$ , and (f)  $\text{Y}_{0.9}\text{CrO}_{3.85}$ . The reduced phases were prepared by reduction with methanol at 543 K for 1 h. The asterisk indicates an unknown band.

The FT-IR spectra of the as-prepared and the reduced phases are shown in Figure 7. Based on the Raman spectra previously reported,<sup>23</sup> absorption bands of the original compounds were assigned as shown in Table 2, where the  $\nu_3$  (antisymmetric-stretching) and  $\nu_1$  (symmetric-stretching) modes of  $\text{CrO}_4^{3-}$  tetrahedra are usually IR-active but the  $\nu_2$  (symmetric-bending) and  $\nu_4$  (antisymmetric-bending) modes are absent or very weak.<sup>33</sup> The spectra for the reduced phases of  $\text{NdCrO}_4$  and  $\text{Y}_{0.9}\text{CrO}_{3.85}$  were quite different from those for the as-prepared ones. As summarized in Table 2, both showed strong absorption bands of O–H bending around 1020–1100  $\text{cm}^{-1}$  and O–H stretching around 3250–3520  $\text{cm}^{-1}$ . The intensity of the bands from the H–O–H bending mode around 1650  $\text{cm}^{-1}$  was so small that it may be assumed that  $\text{H}_2\text{O}$  was present only in trace amounts in both compounds. The TG curves in Figure 6 also support this. In addition, there was strong absorption around 520  $\text{cm}^{-1}$  with a shoulder around 630  $\text{cm}^{-1}$  and weak absorption around 890  $\text{cm}^{-1}$ . These features of the reduced phases of zircon-type compounds are similar to the Cr–O stretching modes of “active” chromium hydroxide gels,  $\text{Cr}(\text{OH})_3 \cdot n\text{H}_2\text{O}$ .<sup>34,35</sup>  $\text{Cr}(\text{OH})_3 \cdot n\text{H}_2\text{O}$  have structures formed by octahedral chains of distorted  $\text{CrO}_{6-m}(\text{OH})_m$  units, between which the hydrogen bonds link as  $\text{O}_{5-m}(\text{OH})_m\text{Cr}^{\text{III}}-\text{O}\cdots\text{H}\cdots\text{O}-\text{Cr}^{\text{III}}-\text{O}_{5-n}(\text{OH})_n$ .<sup>34,35</sup> It has been reported that  $\text{Cr}(\text{OH})_3 \cdot n\text{H}_2\text{O}$  shows strong bands of Cr–O stretching at 470 and 530  $\text{cm}^{-1}$  with a shoulder at 620  $\text{cm}^{-1}$  in IR spectra,<sup>35,36</sup> while  $\text{Cr}_2\text{O}_3$  shows strong bands in ranges of 540–600 and 600–720  $\text{cm}^{-1}$ .<sup>37,38</sup> Generally,  $\text{RE}_2\text{O}_3$  shows strong

bands in the 250–490  $\text{cm}^{-1}$  range and at 570  $\text{cm}^{-1}$ ,<sup>36</sup> and  $\text{REOOH}$  and  $\text{RE}(\text{OH})_3$  show strong bands at around 640  $\text{cm}^{-1}$  and in the 100–430  $\text{cm}^{-1}$  range.<sup>38–40</sup> Therefore, it may be concluded that the charge compensation required by the reduction of  $\text{NdCrO}_4$  and  $\text{Y}_{0.9}\text{CrO}_{3.85}$  is effected by hydrogen. The GC measurements indicated that the main products by the reaction with methanol were  $\text{CO}$ ,  $\text{H}_2$ ,  $\text{HCHO}$ , and  $\text{CH}_3\text{CHO}$  in the gas phase. Consequently, it is probable that hydrogen atoms transferred from the methanol to both zircon-type compounds through a dehydrogenation reaction and that this reduced Cr(V) to Cr(III). The IR spectrum for the reduced phase of  $\text{LaCrO}_4$  was very similar to that of the original  $\text{LaCrO}_4$ , except for the appearance of an unknown band at around 467  $\text{cm}^{-1}$ . Taking into account the result in Figure 6, the charge compensation for the reduction of  $\text{LaCrO}_4$  is concluded to be due to Schottky-type defects of the oxide ions.

**In Situ Raman Spectroscopy.** The Raman spectra of rare-earth metal(III) chromates(V) at 543 K are shown in Figure 8. All of these spectra are assigned to the internal modes of a  $\text{CrO}_4^{3-}$  tetrahedron.<sup>23,25</sup> No change in the spectral features was observed between 297 and 543 K, except for an increase in the phonon frequency by the temperature effect. Spectral assignments are shown in Figure 8A.

The Raman spectra of the compounds measured in situ after 1 h of reduction at 543 K are shown in Figure 8B. For all compounds, the vibrational modes of the  $\text{CrO}_4^{3-}$  tetrahedron are degraded and some additional peaks appear by the reduction. The spectra of the reduced phases are not assigned to the vibrational modes of RE–O or RE–O $\cdots$ H units but to those related to the Cr–O or Cr–O $\cdots$ H units because the main peaks in the IR<sup>38–40</sup> and Raman<sup>41</sup> bands of RE(III) oxides/hydroxides appear in the range below 500  $\text{cm}^{-1}$ . The reduced phases of zircon-type compounds show the bands around 620 and 480  $\text{cm}^{-1}$ , indicated by  $\nu_{h1}$  and  $\nu_{h2}$  in Figure 8B. On the basis of the results by IR, both can be identified as Cr–O stretching modes of the  $\text{Cr}^{\text{III}}\text{O}_{6-m}(\text{OH})_m$  moieties. This agrees with the report that  $\text{Cr}(\text{OH})_3 \cdot n\text{H}_2\text{O}$  shows a strong band at 488  $\text{cm}^{-1}$  and that  $\alpha\text{-CrOOH}$  ( $R\bar{3}m$ , trigonal) shows strong bands in the 555–665  $\text{cm}^{-1}$  range of the Raman spectra; the latter also has a structure built from  $\text{Cr}^{\text{III}}\text{O}_6$  layers linked by hydrogen bonds.<sup>42</sup>

With  $\text{Y}_{0.9}\text{CrO}_{3.85}$ , the lattice mode of  $\text{Cr}_2\text{O}_3$ <sup>43</sup> appeared at 550  $\text{cm}^{-1}$  by reduction, but  $\text{YCrO}_3$  was not detected.  $\text{Cr}_2\text{O}_3$  was not detected by XRD, indicating that the amount of  $\text{Cr}_2\text{O}_3$  was very small and/or it was amorphous. The peak intensity of the lattice mode at 550  $\text{cm}^{-1}$  by Raman spectroscopy is so strong<sup>43</sup> that the detection sensitivity to  $\text{Cr}_2\text{O}_3$  is very high.

Two broad Raman bands were observed in all of the reduced phases: one was at the lower wavenumber side of the  $\nu_3$  mode, centered at around 720  $\text{cm}^{-1}$ , and the

(33) Muller, A.; Baran, E. J.; Carer, R. O. *Struct. Bonding* **1976**, *26*, 81.

(34) Avena, M. J.; Giacomelli, C. E.; DePauli, C. P. *J. Colloid Interface Sci.* **1996**, *180*, 428.

(35) Spiccia, L.; Marty, W. *Inorg. Chem.* **1986**, *25*, 266.

(36) Giovanoli, R.; Stadelman, W.; Feitknecht, W. *Helv. Chim. Acta* **1973**, *56*, 839.

(37) Pimentel, G. C.; Sederholm, C. H. *J. Chem. Phys.* **1956**, *24*, 639.

(38) Nyquist, R. A.; Kagel, R. O. *Infrared spectra of inorganic compounds*; Academic Press: Orlando, FL, 1997.

(39) Christensen, A. N. *Acta Chem. Scand.* **1966**, *20*, 896.

(40) Shafer, M. W.; Roy, R. *J. Am. Ceram. Soc.* **1958**, *42*, 563.

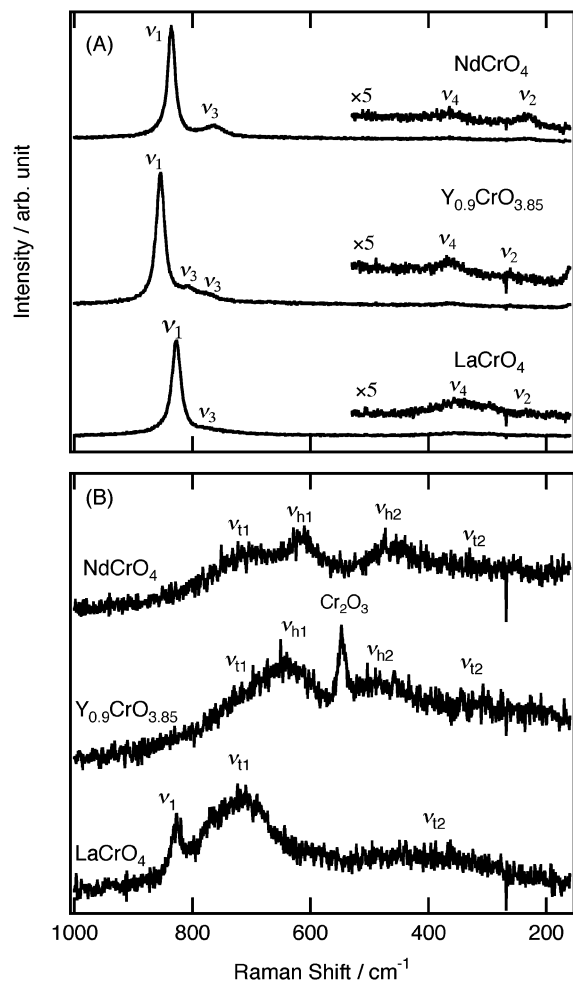
(41) Zeremboitch, J.; Goutheron, J.; Lejus, A. M. *Phys. Status Solidi B* **1979**, *94*, 249.

(42) Maslar, L. E.; Hurst, W. S.; Bowers, W. J.; Hendriks, J. H.; Aquino, M. I.; Levin, I. *Appl. Surf. Sci.* **2001**, *180*, 102.

(43) Farrow, R. L.; Mattern, P. L.; Nagelberg, A. S. *Appl. Phys. Lett.* **1980**, *36*, 212.

**Table 2. IR Bands of NdCrO<sub>4</sub>, Y<sub>0.9</sub>CrO<sub>3.85</sub>, and LaCrO<sub>4</sub> and the Phases Reduced by the Reaction with Methanol at 543 K for 1 h**

		NdCrO <sub>4</sub>	Y <sub>0.9</sub> CrO <sub>3.85</sub>	LaCrO <sub>4</sub>
As-Prepared				
Cr <sup>VO</sup> <sub>4</sub> <sup>3-</sup>	$\nu_2$		542(w)	410(w)
	$\nu_4$	420(w)	795(s)	730(s), 809(s)
	$\nu_3$	782(s)	879(sh)	908(sh)
	$\nu_1$	857(sh)		
Reduced Phase				
Cr <sup>III</sup> O <sub>6-m</sub> (OH) <sub>m</sub> moiety	Cr–O stretching	521(s), 634(sh)	536(s), 635(sh)	
	O···H–O bending	491(sh)	476(sh)	
	O···H–O stretching	1021(s)	1045(s), 1086(sh), 1122 (sh)	
Cr <sup>VO</sup> <sub>4</sub> <sup>3-</sup>	$\nu_3$	3238(m), 3485(sh), 3519(s)	3255(w), 3427(s), 3513(sh)	729(w)
	$\nu_1$			881(b)
unknown				467(b)

**Figure 8.** (A) Raman spectra of as-prepared rare-earth metal(III) chromates(V) at 543 K in air and (B) spectra of the reduced phases measured in situ after 1 h of reduction with methanol at 543 K.  $\nu_1$  mode of the residual LaCrO<sub>4</sub>.

other much broader and ranging from 180 to 530  $\text{cm}^{-1}$ . They are indicated as  $\nu_{t1}$  and  $\nu_{t2}$  in Figure 8B.  $\nu_{t2}$  is distinguishable in the reduced LaCrO<sub>4</sub> at 190–530  $\text{cm}^{-1}$  but very ambiguous in the reduced NdCrO<sub>4</sub> and Y<sub>0.9</sub>CrO<sub>3.85</sub>. The reduced LaCrO<sub>4</sub> contained Cr<sup>III</sup>–O moieties but not Cr<sup>III</sup>–OH moieties and showed only the  $\nu_{t1}$  and  $\nu_{t2}$  modes. Usually, Cr(III) states prefer an octahedral coordination with oxide ions,<sup>44</sup> but the  $\nu_{t1}$  and  $\nu_{t2}$  modes are quite different from the typical vibrational modes

of the octahedral Cr<sup>III</sup>O<sub>6</sub> moieties. It is speculated that  $\nu_{t1}$  and  $\nu_{t2}$  are the vibration modes related to the degraded zircon- and monazite-type structures, but so far the identification of these bands has been withheld because of the lack of supporting data.

In situ Raman spectra were collected during a reduction–oxidation cycle for the three compounds. NdCrO<sub>4</sub> and Y<sub>0.9</sub>CrO<sub>3.85</sub> were reduced with methanol at 543 K for 1 h and then oxidized at 543 K in air for 1 h. The in situ Raman spectra of NdCrO<sub>4</sub> are shown in Figure 9a. By the reduction, the peak intensities of  $\nu_1$ – $\nu_4$  decreased rapidly and the  $\nu_1$  mode disappeared after 17 min, as shown in Figure 9b1. With decreasing intensities of the internal modes of CrO<sub>4</sub><sup>3-</sup>, additional peaks,  $\nu_{h1}$ ,  $\nu_{h2}$ ,  $\nu_{t1}$ , and  $\nu_{t2}$ , appeared simultaneously at around 6 min and the intensities became stable at around 18 min (Figure 9b2). All of these results are consistent with the results by XRD (Figure 1A), indicating that the degradation of NdCrO<sub>4</sub> is caused by hydrogen uptake to form a structure like O<sub>5-m</sub>(OH)<sub>m</sub>Cr<sup>III</sup>–O···H···O–Cr<sup>III</sup>O<sub>5-m</sub>(OH)<sub>m</sub>. By oxidation in air, the  $\nu_{h1}$  and  $\nu_{h2}$  modes weakened rapidly and disappeared at 120 s, while the  $\nu_1$  mode grew quickly (parts c1 and c2 of Figure 9). The  $\nu_{t1}$  mode appears to change to the  $\nu_3$  mode of crystalline NdCrO<sub>4</sub> with increasing intensity. The spectral features after 10 min of oxidation became identical to those of the zircon-type NdCrO<sub>4</sub>, and the intensity of the  $\nu_1$  mode rapidly recovered to about 50% of the original intensity and reached 70% after 1 h. Recovery of the Raman intensity appears to be slower than that of the XRD peaks, but the peak intensity of the XRD pattern is sensitive to the alignment of metal atoms, while the Raman spectrum responds to the strength of Cr–O bonding. Consequently, it is considered that the reduction causes only a little rearrangement of metal atoms, that the perturbation of oxygen atom alignment is larger than that of metal atom alignment, and that the rearrangement of oxygen atoms into a zircon-type structure takes more time.

Parts a and b of Figure 10 are the in situ Raman spectra of Y<sub>0.9</sub>CrO<sub>3.85</sub> during the reduction and oxidation at 543 K, respectively. By the reduction, the  $\nu_1$  mode disappeared after 200 s, and the  $\nu_{h1}$ ,  $\nu_{h2}$ ,  $\nu_{t1}$ , and  $\nu_{t2}$  modes grew rapidly. These results clearly indicate that the degradation of Y<sub>0.9</sub>CrO<sub>3.85</sub> is faster than that of NdCrO<sub>4</sub>. As shown in Figure 10b, the Cr<sub>2</sub>O<sub>3</sub> mode formed during the reduction process did not change by the oxidation. Cr<sub>2</sub>O<sub>3</sub> and YCrO<sub>3</sub> are very stable com-

(44) Cotton, F. A.; Wilkinson, G. *Advanced inorganic chemistry: a comprehensive text*; Wiley: New York, 1980.



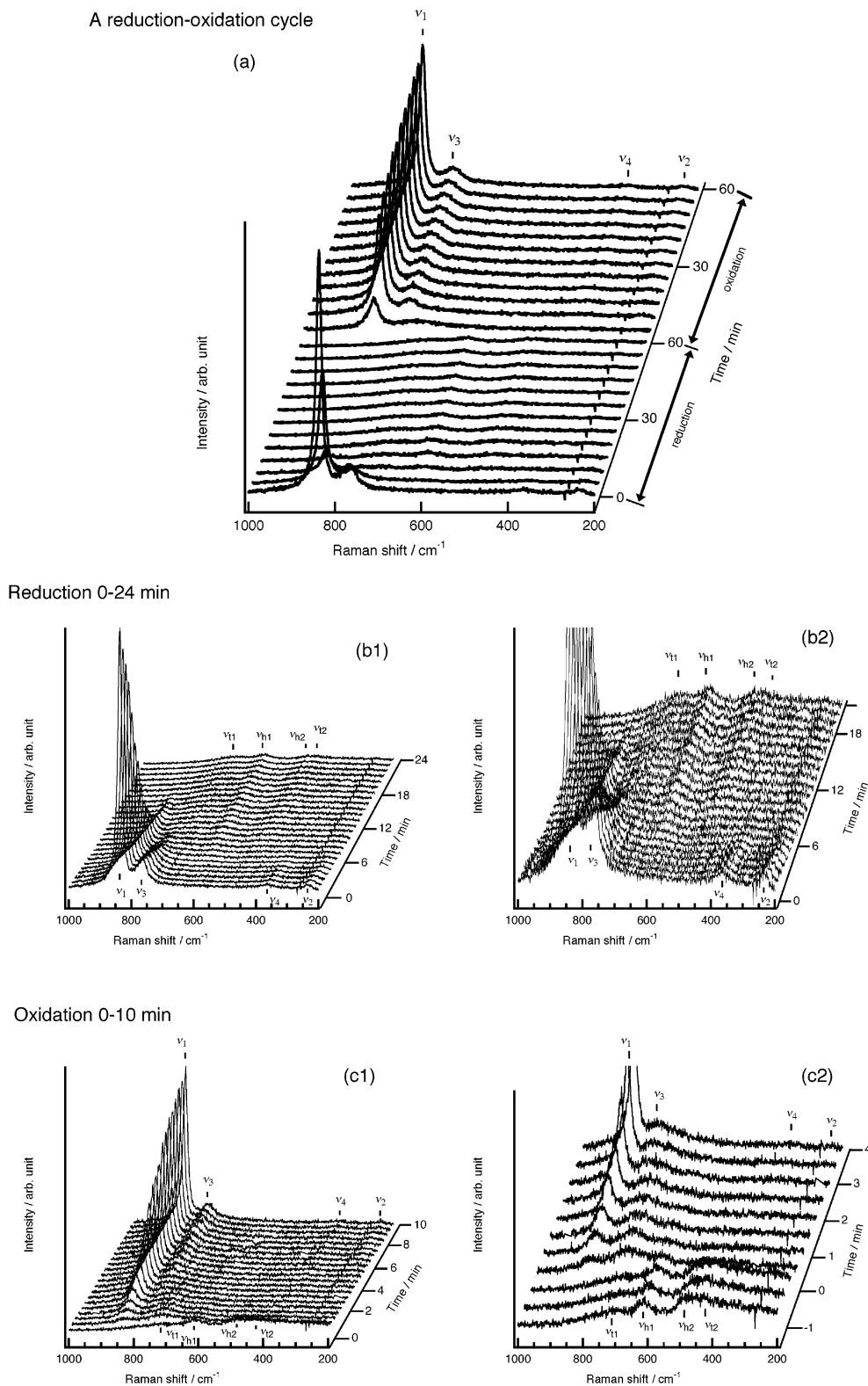


**Figure 9.** In situ Raman spectra of  $\text{NdCrO}_4$  during reduction with methanol at 543 K for 1 h and oxidation at 543 K for 1 h in air: (a) spectral changes over a full cycle; (b1 and c1) details of spectral changes during reduction at 0–24 min and oxidation at 0–10 min, respectively; (b1 and c1) expanded in parts b2 and c2, respectively.

pounds, so that they cannot be oxidized to Cr(V) compounds. It is evident that these compounds hindered the complete restoration of the reduced  $\text{Y}_{0.9}\text{CrO}_{3.85}$  to the original phase.

The Raman spectra of  $\text{LaCrO}_4$  changed by the redox reactions as shown in Figure 11: the reduction continued until the  $\nu_1$ – $\nu_4$  modes had completely disappeared.

The  $\nu_1$  peak did not disappear until 70 min, indicating that the degradation of  $\text{LaCrO}_4$  is much slower than the degradation of the zircon-type compounds. The  $\nu_{11}$  and  $\nu_{12}$  modes appeared by reduction, and they did not change by oxidation at 543 K. A Raman band attributed to the  $\text{Cr}^{\text{III}}\text{—O}\cdots\text{H}$  moiety and  $\text{Cr}^{\text{III}}\text{O}_6$  units was not formed in  $\text{LaCrO}_4$  during the reduction.



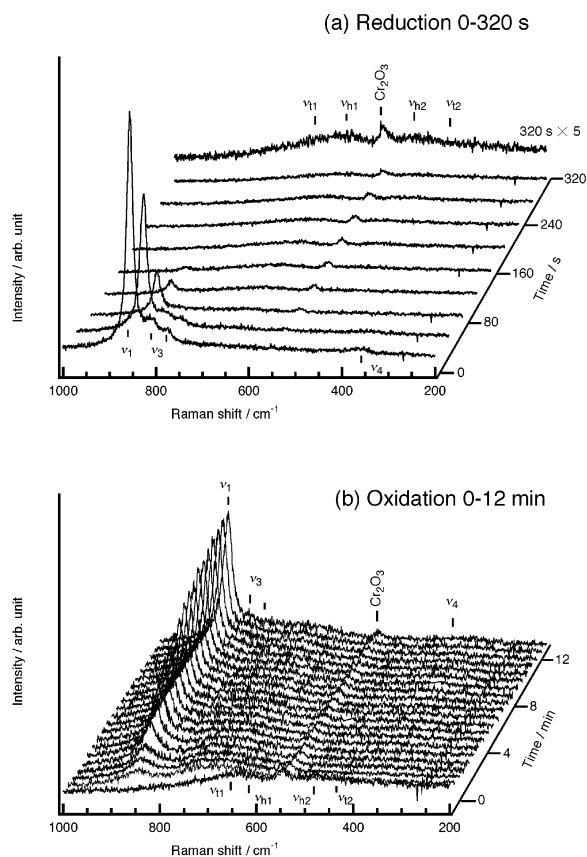


**Figure 10.** (a) In situ Raman spectra of  $Y_{0.9}CrO_{3.85}$  during reduction with methanol at 543 K for 1 h and (b) oxidation at 543 K for 1 h in air.

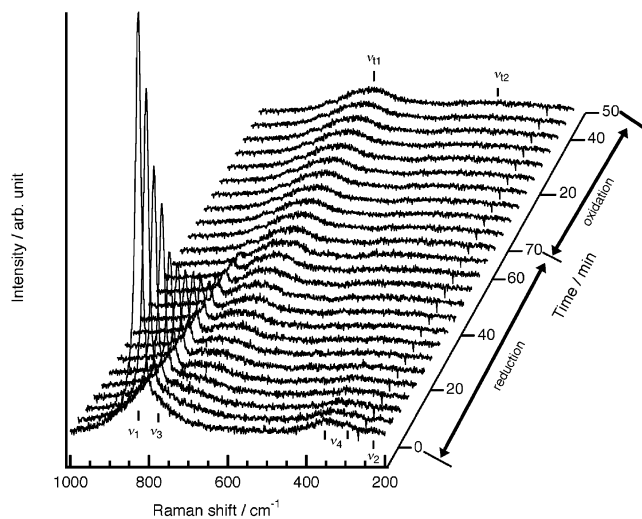


**Figure 11.** In situ Raman spectra of  $LaCrO_4$  during a reduction-oxidation cycle at 543 K.

### Mechanism of the Structural Interconversion.

As mentioned above, only  $NdCrO_4$  showed rapid interconversion between the zircon-type and the low-crystalline, reduced phase at 543 K, and the interconversion of  $NdCrO_4$  is mainly discussed below. The reduction of  $NdCrO_4$  by methanol is considered to occur in the following steps: (1)  $NdCrO_4$  abstracts hydrogen atoms from methanol molecules by the surface reaction, (2) the hydrogen atoms are incorporated into  $NdCrO_4$  by diffusion, (3) Cr(V) is reduced by hydrogen in turn, and (4)  $Cr^{III}O_{6-m}(OH)_m$  moieties are formed. Thus, the final

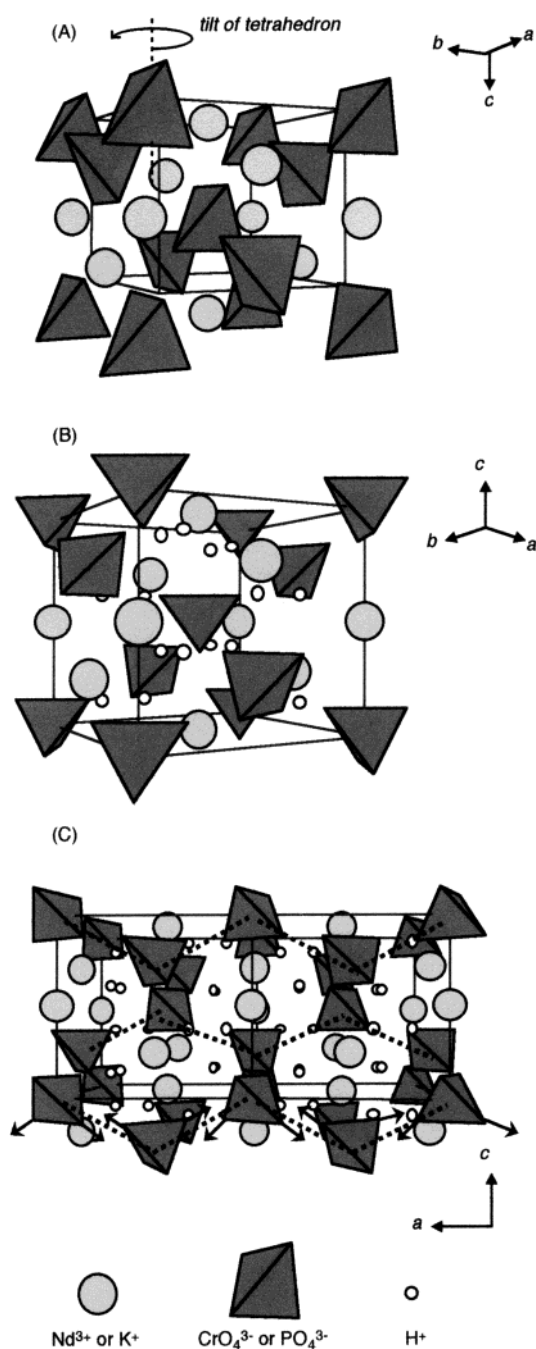


**Figure 12.** Structures of (A) zircon-type  $NdCrO_4$  and (B) tetragonal II- $KH_2PO_4$ . (C) Arrays of the  $AO_4$  tetrahedra in the II- $KH_2PO_4$ -type structure along the  $a$  axis; the dashed bold lines indicate the closest Cr-Cr distances, and the arrows indicate the displacement directions of oxide ions forming the octahedral chain by oxygen-sharing between  $AO_4$  tetrahedra. The frameworks indicate unit cells.

product is postulated to be  $NdH_2CrO_4$ . It must be noted here that the room-temperature phase of  $KH_2PO_4$ , II-KDP ( $I\bar{4}2d$ , tetragonal), bears a structural resemblance to the zircon-type structure.<sup>45,46</sup> Figure 12 shows the structure of  $NdCrO_4$  and II-KDP constructed by using the atomic coordinates in refs 23 and 47, respectively. The arrangement of K and P atoms in II-KDP is the

(45) Hartman, P. *Acta Crystallogr.* **1956**, *9*, 721.

(46) Nyman, H.; Hyde, B. G.; Anderson, S. *Acta Crystallogr., Sect. B* **1984**, *40*, 441.

same as that of Nd and Cr atoms in  $\text{NdCrO}_4$ ; only the positions of oxygen are different. Therefore, as shown in Figure 12, zircon-type  $\text{NdCrO}_4$  can transform to the II-KDP-type phase by tilting the  $\text{CrO}_4$  tetrahedron around the  $c$  direction and bridging through the H atoms at 8d sites between the tetrahedra without rearrangement of metal atoms. Figure 1B shows the XRD pattern of the low-crystalline phase  $\text{NdCrO}_4$  after 1 h of reduction and the pattern of II-KDP calculated by the data in JCPDS 84-1577. Although the peaks of the low-crystalline phase are too broad to be identified exactly, the structural change of  $\text{NdCrO}_4$  is reasonably explained by the transformation to a II-KDP-type phase.

On the basis of the II-KDP structure, Cr(III) ions in the reduced phase are supposed to be present as tetrahedrally coordinated  $\text{H}_2\text{Cr}^{\text{III}}\text{O}_4$  units. However, the reduced  $\text{NdCrO}_4$  also shows Cr–O stretching modes similar to those of  $\text{Cr}(\text{OH})_3 \cdot n\text{H}_2\text{O}$  gels which are built from distorted, octahedral  $\text{CrO}_{6-m}(\text{OH})_m$  units.<sup>35,44</sup> Figure 12C shows the arrays of  $\text{CrO}_4$  tetrahedra along the  $a$  axis in a II-KDP-type structure, where the Cr atoms align at the shortest Cr–Cr distance. By displacement of the two oxide ions of a tetrahedron toward the adjacent tetrahedra, as drawn in Figure 12C, a chain of pseudooctahedral  $\text{CrO}_{6-m}(\text{OH})_m$  units can be constructed in the II-KDP-type structure. Such displacement of oxide ions in some of the tetrahedra in the reduced phase may cause structural degradation and result in the low crystallinity. The mechanism of the conversion of  $\text{NdCrO}_4$  to the low-crystalline phase is summarized by  $\text{NdCrO}_4$  transforming to the II-KDP-type phase by hydrogenation and the fact that the structure of the reduced phase is degraded due to the formation of pseudooctahedral  $\text{CrO}_{6-m}(\text{OH})_m$  moieties by oxygen sharing between some of the  $\text{CrO}_4$  tetrahedra. It has been reported that “active” chromium(III) hydroxide gels are very unstable in ambient atmospheres and that they are easily converted to Cr(VI) oxides by air oxidation.<sup>48</sup> Therefore, it is possible that the distorted  $\text{CrO}_{6-m}(\text{OH})_m$  octahedra formed by the reduction of  $\text{Cr}^{\text{V}}\text{O}_4$  tetrahedra are restored to the original tetrahedra in the bulk scale under mild oxidation conditions.

The XRD pattern of reduced  $\text{Y}_{0.9}\text{CrO}_{3.85}$  and the calculated pattern of II-KDP are shown in Figure 2B, which indicates that  $\text{Y}_{0.9}\text{CrO}_{3.85}$  changes to the low-crystalline II-KDP-type phase by reduction with methanol at 543 K in a manner similar to  $\text{NdCrO}_4$ . Incomplete restoration of this compound is due to the formation of small amounts of  $\text{YCrO}_3$  and  $\text{Cr}_2\text{O}_3$ , which is probably caused by the defect structure.

(47) Tun, Z.; Nelmes, R. J.; Kuhs, W. F.; Stansfield, R. F. D. *J. Phys. C: Solid State Phys.* **1988**, *21*, 245.

(48) Schroeder, S. L. M.; Moggridge, G. D.; Rayment, T.; Lambert, R. M. *J. Phys. VI* **1997**, *7*, 923.

Monazite-type  $\text{LaCrO}_4$  did not change to the II-KDP-type phase by reduction at 543 K because the transformation from a monazite-type to a II-KDP-type phase is very difficult because of the large difference in the arrangement of metal and oxygen atoms. Therefore,  $\text{LaCrO}_4$  changed to an amorphous phase by forming large amounts of Schottky defects of the oxide ions by reduction and did not show a reversible structural change at 543 K.

By separate experiments,  $\text{NdCrO}_4$  was found to show similar interconversion behavior at 543 K by reduction with other alcohols and  $n$ -butane for 3 h and oxidation for 1 h in air. Furthermore, it was confirmed that other zircon-type oxides, such as  $\text{CaCr}^{\text{VI}}\text{O}_4$  and  $\text{NdVO}_4$ , did not show structural changes by the reaction with methanol-saturated  $\text{N}_2$  gas at 623 K for 24 h. These indicate that the unique behavior of zircon-type rare-earth metal(III) chromates(V) is due to the Cr(V) states.

### Conclusion

Reversible structural changes of rare-earth metal(III) chromates(V) occurred by the reaction with methanol and oxidation in air. Zircon-type  $\text{NdCrO}_4$  showed structural degradation by less than 30 min of reduction with methanol at 543 K by changing to a low-crystalline phase. The reduced phase, however, was restored to a zircon-type crystalline phase by oxidation at 543 K for a few minutes in air, even after the crystal structure of  $\text{NdCrO}_4$  was degraded in the bulk scale. During the reaction with methanol,  $\text{NdCrO}_4$  was reduced to Cr(III) by hydrogenation and transformed to the low-crystalline, II-KDP-type phase. This was accomplished by tilting  $\text{CrO}_4$  tetrahedra to form hydrogen bonds between them and resulted in structural distortions due to the formation of pseudooctahedral  $\text{CrO}_{6-m}(\text{OH})_m$  units. This transformation did not involve the rearrangement of metal atoms, so the compound was quickly restored to the original zircon-type phase with the disappearance of hydrogen atoms by oxidation. Defect zircon-type  $\text{Y}_{0.9}\text{CrO}_{3.85}$  was also reduced by hydrogenation and changed (more quickly than  $\text{NdCrO}_4$ ) to the low-crystalline phase, but small amounts of  $\text{YCrO}_3$  and  $\text{Cr}_2\text{O}_3$  were formed by reduction. These compounds were hardly oxidized to the chromate(V) phase, so the structure was not completely restored by oxidation at 543 K for 1 h. Monazite-type  $\text{LaCrO}_4$  did not change to the II-KDP-type phase because of large differences in the structure of the monazite- and II-KDP-type phases. Monazite-type  $\text{LaCrO}_4$  transformed to the amorphous phase by reduction and formed large amounts of Schottky defects in the oxide ions. The reduced  $\text{LaCrO}_4$  was restored to the original crystalline phase at 723 K but not at 543 K.

CM020999K